Power Loss Reductions and Voltage profile improvement through Fuzzy and AO algorithm for effective system operation by optimal placement of UPFC

V. Suryanarayana Reddy[1], A. Immanuel[2], M. Mahesh[3], I. Kumaraswamy[4], P. Vishnuvardhan[5]*

[1]Assistant Professor, Department of EEE, ACET - Gudur, A.P, India
[2]Associate Professor, Department of EEE, ACET - Gudur, A.P, India
[3]Assistant Professor, Department of EEE, AITS – Rajampet, A.P, India
[4]Associate Professor, Department of EEE, Mohan Babu University, Tirupati, A.P, India
[5]Assistant Professor, Department of EEE, ACET - Gudur, A.P, India

Abstract: This project's primary goal is to reduce power losses and improve voltage profiles in power networks by strategically using unified power flow controllers, or UPFCs. The optimization process is enhanced by the combination of Fuzzy Logic and Archimedes Optimization Algorithm (AOA) techniques. The current injection model has been used to optimize the sizing of the Unified Power Flow Controller (UPFC) by the application of the Archimedes optimization method. The suggested approach demonstrates how simple it is to manipulate ideal power flow assessments. Fuzzy systems are used to compute the voltages and power loss at the best places. This paper is a demonstration of how to reduce power loss and enhance voltage under different load scenarios, such as light load, normal load, and overloading cases. It also shows how to apply UPFC to improve system performance on IEE-14 and IEE-30 bus systems.

1 Introduction

In the 1988s, N.G. Hingorani presented the notion for a device called the FACTS stands for Flexible AC Transmission System. More control flexibility is provided by the FACTS devices for dependable and cost-effective power system operation. Gyugyi (1991) [1] provided an explanation of the Unified Power Flow Controller (UPFC) concept among FACTS devices. Technology for flexible AC transmission systems [2] allows for the management of one or more aspects of the AC transmission system, enhancing controllability and power transfer capacity. while restricting voltage and stability with the use of additional static equipment and a power electronic-based system.

The UPFC is utilized for the dynamic compensation and real-time regulation of transmission systems, the UPFC [3] offers the multifunctional flexibility needed to address numerous power delivery issues. The adjective "unified" in the name of the Unified Power Flow Controller [4] designates its unique ability to Control simultaneously the three factors (phase angle, impedance, and voltage) that affect power flow in the transmission line [5]. or selectively within the framework of conventional power transmission concepts. As an alternative, it has the ability to separately regulate the line's actual and reactive power flows. It offers the ability to control any system transmission parameter at the same time.

The two-voltage source back-to-back converters that make up the UPFC are connected via a shunt transformer to a second series converter and a series transformer to a first series converter. A dc storage capacitor provides a common dc link for these two converters to be linked via.

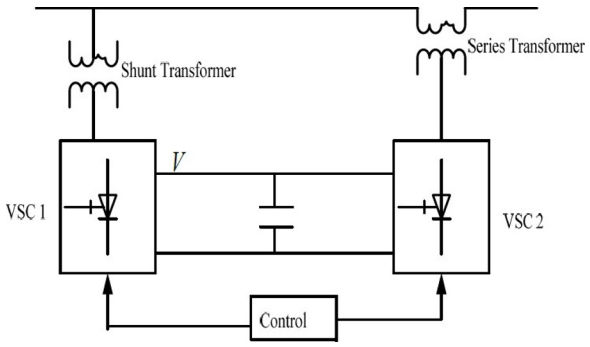

Fig 1: The Schematic diagram of UPFC

Consequently, the goal of Archimedes' optimization technique [6] is to identify the most practical answer to an optimization problem. Consider the global optimum of an n-dimensional function. To determine fitness as well as the global best, or the best value of each particle in the swarm, and personal best, or the best value of individual particle [8], each particle is started at random

* Corresponding author: vemireddysnr@gmail.com

and evaluated using the AO [7] algorithm. After that, a loop starts to find the optimum response. The personal and global bests change the particle's velocity first, then the current velocity updates each particle's position within the loop [9].

2. Literature Review

In 1988, N.G. Hingorani and L. Guygyi provided the first definition of FACTS and FACTS controllers [1]. When we talk about FACTS, we usually mean the utilization of high-power semiconductor devices to control a range of electrical characteristics and parameters, such as currents, phase angles, voltage, resistance, and active and reactive power. Since then, a lot of studies have been conducted in this field utilizing these FACTS devices to improve transmission system power.

The UPFC has been modelled using a variety of modelling approaches [2-4]. In their published works on the susceptance model and firing angle model of SVC [5–6] for the development of power system stability, J. Bian, D. G. Ramey, R. J. Nelson [2], K. K. Sen, and E. J. Stacey [3]

In their study, M. Damodar Reddy and K. Dhananjaya Babu [7] discussed how to best place SVCs by utilizing PSO and fuzzy algorithms. The SVC is modelled in this study as a device that injects reactive power at the bus that it is linked to. Here, the best place for SVC is determined using the fuzzy technique.

The comprehensive power injection model and the adjustments made to the corresponding Jacobian matrix elements in the NR approach for the load flow investigations were reported by A. Meta vural and Mehmattumay [8]. This work derives the power injection equations for the UPFC.

The paper on UPFC control setting by load flow calculation was presented by Ch. Chengaiah, G.V. Marutheswarrao [9]. A presentation on transmission loss allocation and loss minimization by integrating UPFC in load flow analysis was presented by Dr. Shivasharanappa and Sunil Kumar [8].

A study titled "Minimization of losses in transmission networks by incorporating UPFC in load flow studies" was delivered by S.V. Ravi Kumar and S. Siva Nagaraju [10]. This article considers the Hale network, incorporates the UPFC power injection model, and examines power flows for varying UPFC control parameter values.

A differential algorithm strategy for loss reduction by determining the best position for the UPFC and its ideal control parameter setting was presented by R. Vanitha and M. Sudhakaran [11]. This research examines the differences between the UPFC genetic algorithm and differential evolution.

Y. del Valle, J. C. Hernandez, et al. [12] described a step-by-step implementation of the unified power flow controller problem using the particle swarm optimization (PSO) technique (UPFC) sizing and optimal allocation. This study looks into the best way to define PSO parameters, and it tests various power system load scenarios to see how they affect the placement and capacity of each UPFC unit.

The proposed system involves recognizing areas that have not been thoroughly explored or addressed in existing literature. There are Limited comparative studies between PSO and AO in terms of their efficiency, convergence rate, and computational complexity for UPFC placement and Lack of comparative analysis with other optimization techniques such as Genetic Algorithms (GA), Differential Evolution (DE), or Hybrid Methods [9].Since renewable energy sources (RES) have erratic power availability, optimizing their potential requires efficient management. In this instance, a hybrid energy storage system (HESS) is required. Combining hybrid energy storage devices with renewable energy sources can improve power management in a DC micro grid system. For a DC micro grid, this paper suggests the best hybrid energy storage system based on PI controllers to optimize the use of renewable energy sources. The model recommends a particle swarm optimization (PSO) approach to produce an effective PI controller. A 72 W DC micro grid system is taken into consideration in order to verify the efficacy of the suggested optimal PI controller [1].

3. Current Injection Model

The current in the series converter is introduced as a variable via the Current Injection Model [2] (see Fig. 1). The system's limitations for voltage and current are as follows:

Series Voltage: Vs

Impedance of a series transformer: Zs

Impedance of the transmission line: $Z_e^{'}$

$$0.90 \le V_{n,i} \le 1.10 \qquad 0 \le I_{n,ij} \le I_{ij\max}$$

Let's assume that I and j are real and have impedance in the transmission line where the UPFC will be installed is Z_e^i. The UPFC is added to the system by creating the bus bars j and j'.

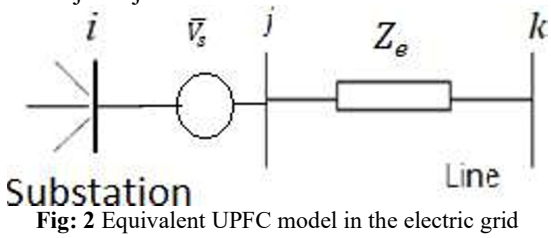

Fig: 2 Equivalent UPFC model in the electric grid

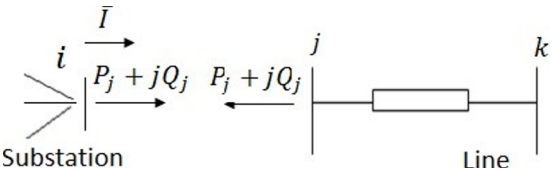

Fig: 3 Power injected as a result of bus bars I and J currents

The equivalent impedance associated to the internal nodes j and j' is erased when the series impedance of the UPFC coupling transformer is $Z_e = Z_e^{'} + Z_e$ and the transmission line are introduced. In Fig. 2, the

corresponding network is shown by π circuits, where bus bars i and j have the series voltage added between them.

3.1 Power injected due to current

The system load's power consumption at US Bar is referred to as S_i^0. Additional power S_i^c and S_j^c, owing to current $\bar{I}$, can be computed with ease using Fig 3. Current $\bar{I}$ introduces two variables i.e, I, φ are associated with the current's module and phase. The current-related power equations are:

$$S_i^c = \overline{V_i}\,\overline{I^*} \qquad S_j^c = -\overline{V_j}\,\overline{I^*}$$

$$P_j^c = -V_j \cos(\varphi - \theta_j),\ Q_j^c = -V_j \sin(\varphi - \theta_j) \quad (2.1)$$

$$P_i^c = -V_i \cos(\varphi - \theta_i),\ Q_i^c = -V_i \sin(\varphi - \theta_i) \quad (2.2)$$

And

$$P_i = P_i^0 + P_i^c,\quad P_j = P_j^c\ \ Q_i = Q_i^0 + Q_i^c,\quad Q_j = Q_j^c \quad (2.3)$$

The new variables φ and I at n and 2n position. The new vector of variables can be written as:

$$\left[x^t\right] = \left[\theta_1, \theta_2 .....\theta_{n-1}, \varphi, V_1, V_2 .....V_{n-1}, I\right]$$

3.2 Series voltage formulas

A model can be created for the UPFC's series voltage equation. One way to express the voltage equation between nodes i and j is as follows:

$$\overline{V_j} - \overline{V_i} = \overline{V_s} \quad (2.4)$$

and the series voltage will be given by,

$$\overline{V_s} = rV_i e^{j\delta} \quad (2.5)$$

where δ denotes the series voltage angle and r is the series voltage factor.

Equation 2.5, when substituted in equation 2.4, will thereafter provide

$$\overline{V_j} - \left(1 + e^{j\delta}\right)\overline{V_i} = 0 \quad (2.6)$$

The complex variable in the typical power flow scenario is if r and δ are constants.

$$A\angle\alpha = -\left(1 + r\angle\delta\right) \quad (2.7)$$

The equation 2.6 can be written as

$$\overline{V_j} + A\angle\alpha \cdot \overline{V_i} = 0 \quad (2.8)$$

The imaginary part Gn = 0 and the real part Fn = 0 respectively

$$F_n = AV_i \cos(\alpha + \theta_i) + V_j \cos(\theta_j) \quad (2.9)$$

$$G_n = AV_i \sin(\alpha + \theta_i) + V_j \sin(\theta_j) \quad (2.10)$$

In an optimization situation, if r and δ are variables, we obtain

$$\left[x^t\right] = \left[\theta_1, \theta_2, ...\theta_{n-1}, \varphi, V_1, V_2, ...V_{n-1}, I, r\right]$$

$$F_n = V_j \cos(\theta_j) - V_i\left[\cos(\theta_i) + \cos(\theta_i + \delta)\right] \quad (2.11)$$

$$F_n = V_j \cos(\theta_j) - V_i\left[\cos(\theta_i) + \cos(\theta_i + \delta)\right] \quad (2.12)$$

The above Fn and Gn are voltage equations.

3.3 Equations for power balance

When a distribution system has 'n' branches, the total power loss is determined by

$$P_{L(total)} = \sum_{i=1}^{n} I_i^2 R_i \quad (2.13)$$

Equation 2.13 depicts the distribution of power between shunt and series converters. Bus I's shunt power will grow due to the series power. With the following formula, let's calculate the power in the series converter.

$$S^S = re^{j\delta}\overline{V_i} I\angle -\varphi \quad (2.14)$$

After dividing the aforementioned equation into active and reactive parts,

$$P^S = rV_i I \cos(\theta_i + \delta - \varphi) \quad (2.15)$$

$$Q^S = rV_i I \sin(\theta_i + \delta - \varphi) \quad (2.16)$$

Active power PS is included in node i.

3.4 Complex Jacobian

The jacobian matrix, with UPFC power addition is given by,

$$J_c^0 = \begin{bmatrix} H^0 & N^0 \\ J^0 & L^0 \end{bmatrix} \quad (2.17)$$

Let's include the voltage equations Fn (2.11) and Gn (2.12) as well as the injected power resulting from current, I bus bar I and j. Complementing the approach is the additional adjustment of the Jacobian matrix caused by the power balance equation.

$$\left[J\right] = \left[J_c^0\right] + \left[J_c\right] + \left[J^s\right] \quad (2.18)$$

The Jacobian matrix resulting from current injection. where the constants δ and r are:

H terms:

$$H_{in}^{c} = \frac{\partial P_i^c}{\partial \varphi} = Q_i^c$$

$$H_{jn}^{c} = \frac{\partial P_j^c}{\partial \varphi} = Q_i^c$$

$$H_{ii}^{c} = \frac{\partial P_i^c}{\partial \varphi} = -Q_i^c$$

$$H_{jj}^{c} = \frac{\partial P_j^c}{\partial \varphi} = -Q_i^c$$

$$H_{ni} = -AV_i \sin(\alpha + \theta_i)$$

$$H_{nj} = -V_i \sin(\theta_i)$$

N terms:

$$N_{in}^{c} = I\frac{\partial P_i^c}{\partial I} = P_i^c$$

$$N_{jn}^{c} = I\frac{\partial P_i^c}{\partial \varphi} = P_j^c$$

$$N_{ii}^{c} = V_i\frac{\partial P_i^e}{\partial V_i} = P_i^c$$

$$N_{jj}^{c} = V_i\frac{\partial P_j^c}{\partial V_i} = P_j^c$$

$$N_{ni} = AV_i \cos(\alpha + \theta_i)$$

$$N_{nj} = V_j \cos(\theta_j)$$

J terms:

$$J_{in}^{c} = I\frac{\partial Q_i^c}{\partial \varphi} = -P_i^c$$

$$J_{jn}^{c} = I\frac{\partial Q_i^c}{\partial \varphi} = P_j^c$$

$$J_{ii}^{c} = \frac{\partial Q_i^c}{\partial \theta_i} = P_i^c$$

$$J_{jj}^{c} = V_i\frac{\partial Q_j^c}{\partial \theta_i} = P_j^c$$

$$J_{ni} = AV_i \cos(\alpha + \theta_i)$$

$$J_{nj} = V_j \cos(\theta_j)$$

L terms:

$$L_{in}^{c} = I\frac{\partial Q_i^c}{\partial I} = Q_i^c$$

$$L_{jn}^{c} = I\frac{\partial Q_i^c}{\partial \varphi} = Q_j^c$$

$$L_{ii}^{c} = \frac{\partial Q_i^c}{\partial \theta_i} = Q_i^c$$

$$L_{jj}^{c} = V_j\frac{\partial Q_j^c}{\partial \theta_i} = Q_j^c$$

$$L_{ni} = AV_i \sin(\alpha + \theta_i)$$

$$L_{nj} = V_j \sin(\theta_j)$$

Modification owing to power balance in Jacobian terminology
H terms:

$$H_{ii}^{s} = \frac{\partial P_s}{\partial \theta_i} = -rV_iI\sin(\theta_i + \delta - \varphi) = -Q^s$$

$$H_{in}^{s} = \frac{\partial P_s}{\partial \varphi} = rV_iI\sin(\theta_i + \delta - \varphi) = Q^s$$

N terms:

$$N_{in}^{s} = I\frac{\partial P_s}{\partial I} = rV_iI\cos(\theta_i + \delta - \varphi) = P^s$$

$$N_{ii}^{s} = V_i\frac{\partial P_s}{\partial V_i} = rV_iI\cos(\theta_i + \delta - \varphi) = P^s$$

The Jacobian, which is no longer a square matrix, alters as follows when r and δ are variables. The above equations use a load flow solution to determine the load flow in transmission networks using commonly used load flow analysis techniques such as Newton-Raphson methods.

Fuzzy logic controller

Principal objectives must be considered. When developing a fuzzy logic to decide the optimal placement for UPFC.

Reducing the amount of power outage and

Keeping the voltage within allowable bounds.

By considering a set of regulations, algorithm for fuzzy inference (FIS) is used to figure out each distribution system node's UPFC placement credibility. To assess the real and reactive power losses in the first stage, the load flow studies for the starting system must be consulted. Again, load flow solutions must be used to balance the total reactive loads at each distribution system node in order to minimize power losses.

The loss reduction is then subjected to linear normalization in the range [0,1], where a value of 1 represents the largest loss drop, while a quantity of 0 suggests the smaller value. The Underneath formula suggests to identify the nth node index power loss value.

$$PLI = \frac{LR(i) - LR(\min)}{LR(\max) - LR(\min)} \quad (4.1)$$

& $$LR_i = P_i^1 - P_i^2 \quad (4.2)$$

Where i= 1 to number of load buses

LRi = loss reduction

P_i^1 = Actual power for a typical load.

P_i^2 = Actual power for load flow and total reactive load correction at the ith node.

Equations 4.1 and 4.2 normalize the LR input so that the values fall between 0 and 1. where 0 will be assigned to the smallest value and 1 to the highest. The optimal buses have been identified using the fuzzy approach, and branches that are in relation to these optimal buses are taken into consideration for UPFC placement.

Node voltages (V) per unit are examples of input variables, whereas UPFC suitability index (UPFC-SI) and index (PLI) are examples of outputs variables. PLI ranges from 0 to 1, while the voltage range of the PU Node is between 0.9 and 1.1. The UPFC SI output variable has a range of 0 to 1. For PLI, five triangle membership functions are displayed in. All five membership features—L, LM, M, H, and HM—are displayed in Figure 4.

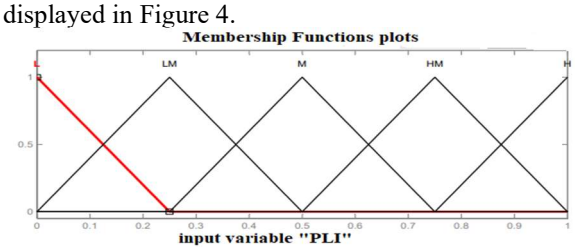

Fig: 4 Membership PLI functions

Five membership functions were chosen for tension are shown in Fig.5. The membership functions that are trapezoidal and triangular are L, LM, M, HM, and H. For DSTATCOMSI, these five triangle functions have been chosen. L, HM, M, LM, and H are those.

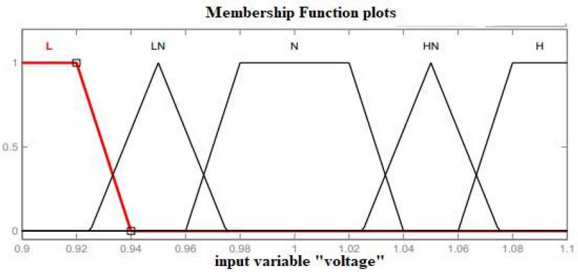

Fig:5 Voltages membership functions

Five membership functions were chosen for tension. These are L, LM, M, HM and H. The Fig 5. Shows triangular and Trapezoidal membership functions. Five triangular membership functions are selected for UPFCSI. Fig 6 shows the five functions of L, M, LM, H and HM.

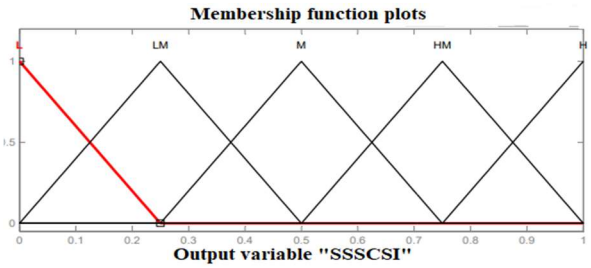

Fig: 6 Membership functions for SSSCSI

Rules must be developed to asses a node's suitability for DSTATCOM installation in order to design the best location for the device within Fuzzy. Fuzzy's rules table as shown in table :1

Table :1 Table of rules for FLC design

And		Voltage				
		L	Lm	m	Hm	H
PLI	L	Lm	Lm	L	L	L
	Lm	M	Lm	Lm	L	L
	m	Hm	M	Lm	L	L
	Hm	Hm	Hm	M	Lm	L
	H	H	Hm	M	Lm	Lm

These rules are in following format :

- if voltage is L and PLI is H, then UPFC-SI is H.
- If voltage is N and PLI is M, then UPFC-SI is Lm.
- If voltage is H and PLI is H, then UPFC-SI is Lm.

The terms "if" and "then" in a rule are called rule-antecedent and rule-consequent, respectively, in this context. For two inputs and five membership functions, twenty-five rules have been formed.

Archimedes Optimization Technique

The Archimedes Optimization Algorithm (AOA) is an innovative metaheuristic optimization technique inspired by the principles of buoyancy and fluid mechanics, rooted in Archimedes' laws of physics. This algorithm has shown promise in solving complex optimization problems across various domains. The ideal positioning of Unified Power Flow Controllers (UPFCs) within power systems is one of the noteworthy uses of AOA.

An innovative optimization approach called AOA was put forth to address issues in the actual world (Hashim et al., 2020b). This optimizer draws influence from the principles of Archimedes. It depicts how force behaves when an object is either fully or partially dipped in a liquid. Similar to the majority of metaheuristic algorithms and swarm optimizers, AOA suggests population-based solutions. The things that are submerged in this case indicate the offered solutions. Objects, locations, and solutions are among the first set of random parameters that are suggested at the start of the optimization process. Each particle has a unique acceleration, density, and volume that are updated over repeated cycles. The following is the process for upgrading the AOA.

Algorithm steps

Unlike other optimizers, the AOA takes into account both exploration and exploitation, hence it can be classified as a global optimizer. Among the mathematical stages in the AOA are initialization, objective function evaluation, and parameter update.

The following procedures are detailed in detail :
Step :1 Initialization :
As in equation 5.1, provide a starting set of positions for the entire population.

$$O_i = lb_i + rand \times (ub_i - lb_i); i = 1,2....N \quad (5.1)$$

In a population set of N solutions, Oi stands for the ith solution. The search-space's bottom and upper bounds are denoted by lbi and ubi, respectively.
The volume (vol) and density (den) for every ith solution are initialized using equation 5.2.

Deni = rand (Pbest)
Voli = rand (Gbest) (5.2)
Where the variable rand is a random vector of Dim dimension with values between 0 and 1. Equation 5.3 displays the ith solutions initial acceleration (acc).

$$acc_i = lb_i + rand \times (ub_i - lb_i) \quad (5.3)$$

Selecting the best-valued response entails assessing the goal (fitness) function.For the minimization or maximization problems, the optimum value is the lowest or largest, respectively.Assign the following : $xbest$, $denbest$, volbest and $accbest$.

Step 2- Update densities, volumes :
Next, using equation 5.4 as a guide, the density and volume of solution I in iteration t+1 are adjusted.

$$den_i^{t+1} = den_i^t + rand \times (den_{best} - den_i^{'})$$
$$vol_i^{i+1} = vol_i^t + rand \times (vol_{best} - vol_i) \quad (5.4)$$

In this case, V and D are the global solutions volume and density, and y is a random value between 0 and 1.

Step 3- Normalize acceleration :

Equation (5.5) is used to normalize the acceleration and calculate the percentage of change.

$$acc_{i-norm}^{t+1} = u \times \frac{acc_i^{t+1} - \min(acc)}{\max(acc) - \min(acc)} + l \quad (5.5)$$

where the values of 0.9 and 0.1 represent the upper and lower normalization ranges, indicated by the symbols u and l, respectively. A $acc_{i,normal}^{i+1}$ establishes the adjusting each agent's step %. An item is said to be in the exploratory state and distant from the ideal solution if its acceleration value is high. If not, the object is moved to the state of exploitation. Typically, an acceleration begins at a high number and then progressively drops as one step moves into the next. This approach avoids getting trapped in local areas and instead lets the solutions flow toward the global best, achieving equilibrium between the exploration and exploitation phases.

Step 5- Update Position :

If T F ≤ 0.5 (exploration phase), the ith objects position is updated for the next iteration t+1 using equation (5.6)

$$x_i^{t+1} = x_i^t + C_1 \times rand \times acc_{i-norm}^{t+1} \times d \times (x_{rand} - x_i^t) \quad (5.6)$$

Where C1 is a constant value of 2. Otherwise, if T F>0.5 (exploitation phase), the solutions are updating their locations according to following equation.

$$x_i^{t+1} = x_{best}^t + F + C_1 \times rand \times acc_{i-norm}^{t+1} \times d \times (T \times x_{rand} - x_i^t)$$

Where the constant value $C2$ is 6. A variable that increases is T. It is proportionate to the transfer operator and a function of time. One way to compute it is by using $T = C3 \times T\ F$. Initially, T takes up a certain proportion of the ideal site, and this percentage increases with time in the range [$C3$ × 0.3, 1]. It starts with a small percentage and increases the random walk's step-size with time. The distance to the global answer gets smaller as this proportion rises.

The Fig 7 shows flow chat of Archimedes Optimization Algorithm technique.

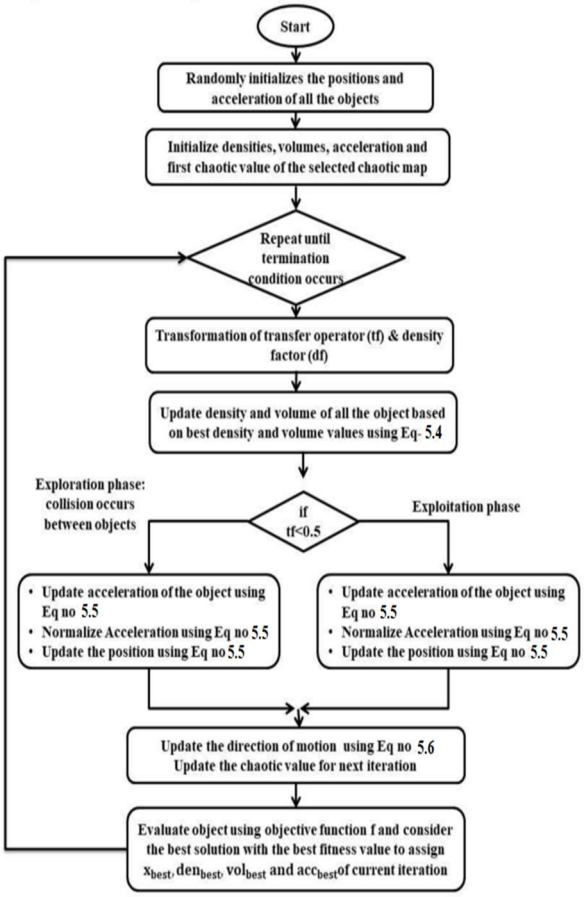

Fig :7 Flow chart of AOA

Results
For the goals under consideration, the suggested technique approach is utilized to position the UPFC on the node with the lowest voltage profile and largest loss reduction, as will be covered in the section that follows.

6.1 Results of 14 bus system :

The IEEE 14 bus system [10] is made up of 20 transmission lines, 5 generator buses (numbers 1, 2, 3, 6, and 8), and 9 load buses (numbers 4, 5, 7, 9, 10, 11, 12, 13, and 14). There are several load circumstances, such as under load (<100%), normal load (=100%), and

overload (>100%). The task at hand involves determining the ideal bus number and UPFC (current in P.U.) rating in conjunction with the current injection model. In this instance, the PSO is able to determine the UPFC's rating. Tables 2 present the simulation findings for optimal locations and power loss reduction before and after the placement of the UPFC.

Table 2: Results for IEEE 14 bus system

Loading condition	Losses without UPFC (MW)	UPFC Location	AOA Losses with UPFC
Normal loading	13. 3938	14, 13	12.3196
Under loading	8.0728	5, 4	7.0488
Over loading	16.7223	14, 9	15.4393

The fig.8 shows the testing results before and after placement of UPFC at normal loading condition at 14-bus system.

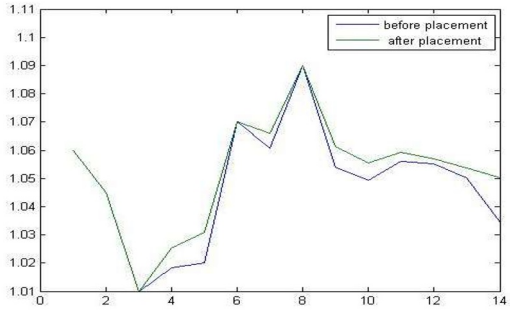

Fig: 8 Voltage profile for normal loading (100%), both before and after the UPFC is placed.

Under typical loading conditions (normal loading condition), the 13th and 14th bus is the best place for UPFC to be. The losses were 13.3938 MW prior to the installation of the UPFC, and they will drop to 12.3196 MW following the UPFC.

The fig.9 shows the testing results before and after placement of UPFC at under loading condition (<100%) at 14-bus system.

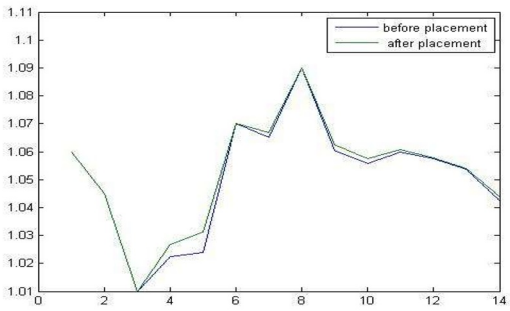

Fig: 9 Voltage profile for under loading (<100%) before and after UPFC implantation.

Under typical loading conditions (under loading condition), the 4th and 5th bus is the best place for UPFC to be. The losses were 8.0728MW prior to the installation of the UPFC, and they will drop to 7.0488 MW following the UPFC.

The fig.10 shows the testing results before and after placement of UPFC at over loading condition (>100%) at 14-bus system.

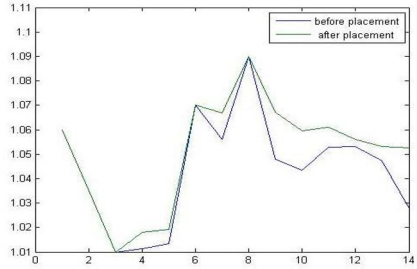

Fig: 10 Voltage profile for overloading (>100%) before and after UPFC placement.

Under typical loading conditions (over loading condition), the 9th and 14th bus is the best place for UPFC to be. The losses were 16.7223 MW prior to the installation of the UPFC, and they will drop to 15.4393 MW following the UPFC.

6.2 Results of 30 bus system:

There are five generators, forty-one transmission lines, and one slack bus in the test system. The generator manages the voltage. These generator buses are not included in the AOA search process since they do not require a UPFC. The task at hand involves determining the best bus number and location for UPFC (current in P.U.). Using the injection model that is in use now. In this instance, the AOA is able to determine the UPFC's rating. Tables 3 present the simulation findings for optimal locations and reduction of power loss both before and after the UPFC is installed.

Table 4: Results for IEEE 30 bus system

Loading condition	Losses without UPFC (MW)	UPFC Location	PSO Losses with UPFC (MW)
Normal Loading	17.528	21 24 30	16.3568
Under Loading	12.1131	26 21 7	11.0155
Over loading	21.9318	21 24 26	20.7544

Figure 11 displays the testing results for the 30-bus system before and after the UPFC was installed under typical loading conditions.

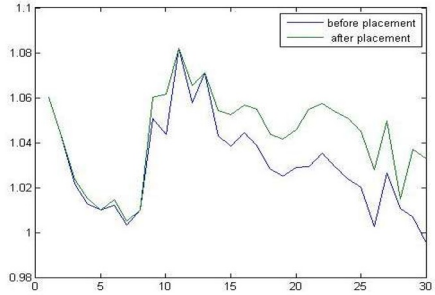

Fig: 11 Voltage profile for normal loading (100%), both before and after the UPFC is placed.

Under typical loading conditions (normal loading condition), the 21th, 24th and 30th bus is the best place for UPFC to be. The losses were 17.528 MW prior to the installation of the UPFC, and they will drop to 16.3568 MW following the UPFC.

The fig.12 shows the testing results before and after placement of UPFC at under loading condition (<100%) at 30-bus system.

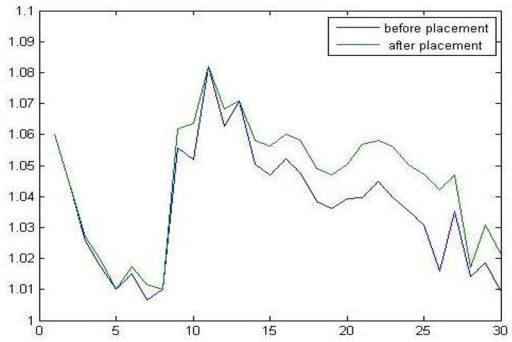

Fig: 12 Voltage profile for under loading (<100%) before and after UPFC implantation.

Under typical loading conditions (under loading condition), the 7th, 21st and 26th bus is the best place for UPFC to be. The losses were 12.1131MW prior to the installation of the UPFC, and they will drop to 11.0155 MW following the UPFC.

The fig.13 shows the testing results before and after placement of UPFC at over loading condition (>100%) at 30-bus system.

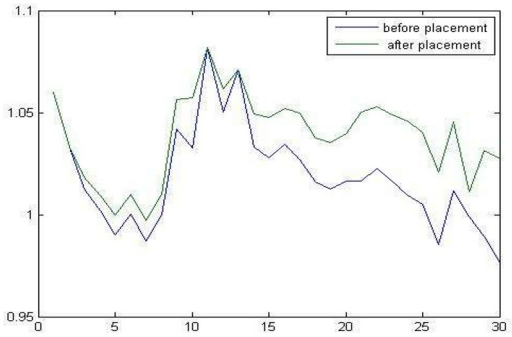

Under typical loading conditions (over loading condition), the 21st, 24th and 26th bus is the best place for UPFC to be. The losses were 21.9318 MW prior to the installation of the UPFC, and they will drop to 20.7544 MW following the UPFC

7. Conclusion

This project's primary goal is to better understand the intricate field of precisely setting up Unified Power Flow Controllers (UPFCs) to lower power losses and improve voltage profiles in order to operate power systems that are more dependable, adaptive, and efficient. The Fuzzy Logic Controller in conjunction with the Archimedes Optimization algorithm (AOA) proved to be a dependable method for handling the intricacies present in power distribution networks. The meticulous research for the project included multiple significant phases. First, the focus was on understanding the fundamental components of the power system and the significance of minimizing power losses and preserving a constant voltage profile. It became evident that implementing cutting-edge technologies like UPFC is essential to achieving these objectives.

The IEEE 14 bus system has a power loss reduction of 12.3196, while the IEEE 30 bus system has a power loss reduction of 16.3568. This suggests that both the system's power losses and voltage profile have improved and risen within the given parameters.

References

1. Ch. Naga Sai Kalyan; B. Srikanth Goud; H. Kishan; Punyavathi Ramineni; B. Praveen Kumar; T. Anil Kumar, “Donkey and Smuggler Optimization Algorithm-based Degree of Freedom Controller for Stability of Two Area Power System with AC-DC Links”, 02 March 2023 ISBN Information: DOI: 10.1109/ICRAIE56454.2022.10054318.
2. Ramanjaneya Reddy Udumula, Tarkeshwar Mahto, Ch Naga Sai Kalyan Optimal PI-Controller-Based Hybrid Energy Storage System in DC Microgrid, ournal: Sustainability, 2022, Volume: 14, Number: 14666.
3. Glover, J. D., Sarma, M. S., & Overbye, T. J. (2021). Power System Analysis and Design. Cengage Learning.
4. Akagi, H. (2019). Control Strategy of Active Power Filters Using Multiple Voltage-Source PWM Converters. IEEE Transactions on Industrial Applications, 41(5), 1322-1331.
5. Hossain, M. A., & Tamura, J. (2020). Fuzzy Logic-Based Load-Frequency Control of Hydrothermal Power Systems. IEEE Transactions on Energy Conversion, 10(2), 299-305.
6. Kennedy, J., & Eberhart, R. (2022). Particle Swarm Optimization. In Proceedings of IEEE International Conference on Neural Networks (Vol. 4, pp. 1942-1948).
7. Dash, P. K., & Subudhi, B. (2018). Optimal placement of FACTS devices for congestion management using particle swarm optimization. Electric Power Systems Research, 78(6), 975-983.
8. Wood, A. J., Wollenberg, B. F., & Sheble, G. B. (2020). Power Generation, Operation, and Control. John Wiley & Sons.
9. Singh, B., Chandra, A., & Al-Haddad, K. (2017). A review of active filters for power quality improvement. IEEE Transactions on Industrial Electronics, 54(4), 1002-1016.
10. Saeedeh Torabi Jafrodi, Mojgan Ghanbari, Mehrdad Mahmoudian, Arsalan Najafi, Eduardo M. G. Rodrigues and Edris Pouresmaeil, A Novel Control Strategy to Active Power Filter with Load Voltage Support Considering Current Harmonic Compensation, Appl. Sci. 2020, 10(5), 1664; https://doi.org/10.3390/app10051664
11. C. N. Sai Kalyan, B. Srikanth Goud, H. Kishan, P. Ramineni, B. P. Kumar and T. Anil Kumar, "Donkey and Smuggler Optimization Algorithm-based Degree of Freedom Controller for Stability of Two Area Power System with AC-DC Links,"

2022 IEEE 7th International Conference on Recent Advances and Innovations in Engineering (ICRAIE), MANGALORE, India, 2022, pp. 461-466, doi: 10.1109/ICRAIE56454.2022.10054318, https://ieeexplore.ieee.org/abstract/document/10054318

12. Maya Vijayan, Ramanjaneya Reddy Udumula, Ch Naga Sai Kalyan, B Srikanth Goud, Bhamidi Lokeshgupta, Optimal PI-Controller-Based Hybrid Energy Storage System in DC Microgrid, https://doi.org/10.3390/su142214666
13. 11). B. Praveen Kumar, M. Saravanan, S. Cynthia Christabel, Robust detection of real-time power quality disturbances under noisy condition using FTDD features, https://hrcak.srce.hr/hr/clanak/348020%3F
14. Duong Quoc Hung and Nadarajah Mithulananthan, "Multiple Distributed Generator Placement in Primary Distribution Networks for Loss Reduction" , IEEE Trans on Industrial electronics, vol. 60, no. 4, April 2013.
15. N. Acharya, P. Mahat, and N. Mithulananthan, “An analytical approach for DG allocation in primary distribution network,” Int. J. Elect. Power Energy Syst., vol. 28, no. 10, pp. 669–678, Dec. 2006.
16. H. L. Willis, “Analytical methods and rules of thumb for modeling DG distribution interaction,” in Proc. IEEE Power Eng. Soc. Summer Meet., 2000, vol. 3, pp. 1643–1644.